Copper Phosphotungstate-Catalyzed Microwave-Assisted Synthesis of 5-Hydroxymethylfurfural In A Biphasic System

Gabriel Abranches Dias Castro
Universidade Federal de Viçosa
Neide Paloma Gonçalves Lopes
Universidade Federal de Viçosa
Sergio Antonio Fernandes
Universidade Federal de Viçosa
Márcio José da Silva (silvamj2003@ufv.br)
Universidade Federal de Viçosa https://orcid.org/0000-0003-0060-0551

Research Article

Keywords: Biorefinery, 5-hydroxymethylfurfural, Keggin heteropoly salts, carbohydrates, microwaves.

Posted Date: December 2nd, 2021

DOI: https://doi.org/10.21203/rs.3.rs-1104511/v1

Abstract

In this paper, we have described a novel route to produce 5-hydroxymethylfurfural (HMF), a valuable platform-molecule obtained from biomass, using transition metal-exchanged Keggin heteropolyacid salts as catalysts, in microwave-assisted reactions carried out in a water-ethyl acetate biphasic system. To avoid the use of homogenous Brønsted acid catalysts, which are corrosive and difficult to be reused, we have exchanged the protons of the Keggin heteropolyacids by transition metal cations. These salts were evaluated in the fructose dehydration, being the $Cu_{3/2}PW_{12}O_{40}$ the most active and selective catalyst, achieving 81 % of HMF yield, after 15 min reaction at 413 K under microwave irradiation (MWI). The effects of metal cation, anion, and heteropolyanion present in the catalyst were evaluated. The greatest efficiency of $Cu_{3/2}PW_{12}O_{40}$ was attributed to its high Lewis acidity strength, which allows that it coordinate with water molecules, consequently generating H_3O^+ ions in the reaction medium. Even though the catalyst has been water-soluble, it was easily reused removing the extracting phase, and adding a new load of the substrate to the remaining aqueous phase. This way, it was successfully reused without loss activity.

1. Introduction

The required reduction of the dependence on fossil-origin products has stimulated the source for renewable raw materials, which can be transformed to biofuels and or high-value-added chemicals in processes with low environmental impacts [1–3]. In this sense, biomass-derivative feedstocks rise as the best alternative to provide substitutes to the petrochemical origin products. Abundant and renewable biomass resources can be converted to platform molecules, which by your turn can generate fine chemicals or biofuels [4–7].

Among them, 5-hydroxymethylfurfural (HMF) is one of the “top 10” biobased chemicals by the U.S. Department of Energy as a platform for value-added products. HMF deserves to be highlighted due to its numerous applications such as solvents, bio-polymers, medicines, personal care products [8,9]. It is a chemical platform that can be obtained through acid-catalyzed dehydration of carbohydrates and thus converted into biofuels, fuel additives, agrochemicals, pharmaceuticals, resins, polyesters, among other useful products [10–12].

Although a plethora of catalytic systems has already been explored to synthesize HMF, there are still many challenges to be overcome before they become environmentally and economically viable [13,14]. Particularly, finding an efficient, inexpensive, and environmentally friendly organic solvent to extract the HMF has been a goal pursued [15]. Dimethyl sulfoxide has been used in numerous works, with excellent yields, but its separating from HMF is a very complicated procedure, due to its high boiling point (189 °C) [16,17]. Ionic liquid-based systems are also explored, there are still several challenges to making these systems economically and environmentally feasible processes for HMF production [18]. Some authors have attempted to convert carbohydrates to HMF in water, but the formation of humins due to condensation of HMF molecules, and the side-reaction of rehydration of the furan ring leading to the

formation of levulinic acid can compromise the selectivity reaction. Therefore, the use of biphasic systems is an attractive alternative, since the conversion of carbohydrate to HMF occurs in the aqueous phase and it can be instantly extracted to another phase, preventing parallel reactions, and eliminating purification steps [19–21]

Keggin-type heteropolyacids (HPAs) are widely exploited catalysts in acid-catalyzed reactions [22–25]. Recently, they have been successfully used in the conversion processes of biomass derivatives platform molecules into high value-added products [26,27]. Similarly, Keggin HPAs have been also used as catalysts to convert hexoses into platform molecules. For instance, phosphotungstic acid, the strongest Brønsted acid among the Keggin heteropolyacids, has been used as a catalyst to produce HMF from different carbohydrates molecules [28].

However, the low surface area and the solubility of Keggin HPAs in polar solvents makes the recovery process laborious, and to circumvent this drawback, they have been supported or anchored on solid matrices such as mesoporous silica, or different mixtures of metal oxides [29–33].

The main challenge for solid-supported HPAs is to resist the leaching triggered by high medium polarity. An approach that has achieved noticeable results is the total or partial exchange of the protons belonging to the Keggin heteropolyacids by large metal cations such as Potassium or Cesium [34–37]. This transformation makes these heteropolyacids insoluble salts which have been demonstrated to be highly efficient catalysts [38].

On the other hand, when the metal cation is a Lewis acid likewise Sn(II) cations, the activity of the catalyst may be considerably improved [39–41]. Recently, Tin(II) silicotungstate was successfully used in the synthesis of alkyl levulinates from different carbohydrates [42]. However, in that work the reaction was carried out at a conventional heating system (ca. 433 K), in a homogeneous system (i.e., alkyl alcohol), hampering the product's purification step.

In this work, we evaluate the catalytic activity of transition metal-exchanged HPAs catalysts in the production of HMF in microwave-assisted (MW) reactions carried out in a water-ethyl acetate biphasic system. In this system, heteropoly salt remained soluble in water, since that the cations selected have small ionic radium. Since that the characterization of the catalysts was previously published [43], the focus herein was mainly to evaluate the impacts of the main reaction variables in the HMF yielding as well as to establish a mechanism that can explain the catalytic results.

2. Experimental

2.1. Chemicals

All reagents, solvents and analytical standards were acquired from commercial sources and used without previous treatment. The hydrated HPAs (i.e., $H_3PW_{12}O_{40}{\cdot}n\ H_2O$, $H_3PMo_{12}O_{40}{\cdot}n\ H_2O$ e $H_4SiW_{12}O_{40}{\cdot}n\ H_2O$; (99.9 wt %)) were purchased from Sigma-Aldrich. All the metal salts, $CrCl_3{\cdot}6H_2O$ (98 wt. %), $FeCl_3{\cdot}6\ H_2O$

(97 wt. %), $AlCl_3 \cdot 6\ H_2O$ (99.5 wt. %), $CuCl_2 \cdot 2\ H_2O$ (99 wt. %), $MnCl_2 \cdot 4\ H_2O$ (99 wt. %), $CoCl_2 \cdot 6\ H_2O$ (98 wt. %), and $NiCl_2 \cdot 6\ H_2O$ (97 wt. %) were Vetec.

2.2. General procedure for the synthesis of heteropoly salts

The general procedure for the synthesis of heteropoly salt catalysts exchanged with transition metals was carried out via heteropolyacid acid metathesis with a dilute solution of the metal chlorides, as described in the literature [43]. Typically, a solution of HPA (ca. 1 g) was dissolved in water (ca. 30 mL) and to this solution, another one containing the desired metal chloride in a stoichiometric amount was slowly added, dropwise under constant magnetic stirring. Afterwards, the resulting solution was heated to 343 K and magnetically stirred for 3h Subsequently, the solution was evaporated releasing HCl and providing the solid salt, which was dried at 383 K for 3h.

2.3. Heteropoly salts characterization

To check the success of synthesis, the catalysts were characterized by infrared spectroscopy analysis (FT-IR/ ATR Varian 660-IR spectrometer). The measurements of the acidity strength of the catalysts were carried out through the measurement of the initial electrode potential (ie Bel, model W3B) in an acetonitrile solution containing the soluble heteropoly salt. Potentiometric titration was performed to estimate the number of acidic sites. The procedure was performed according to the work described by [44]. Typically, 50 mg of salt was dissolved in CH_3CN (30 mL), magnetically stirred for 3 h at room temperature. Subsequently, the content was titrated with a solution of n-butylamine in acetonitrile (ca. 0.025 mol L^{-1}). These data are presented in the supplemental material (Figs. 1SM to 11SM).

2.4. General procedure for the synthesis and quantification of HMF

In a Pyrex glass tube, fructose (0.25 mmol) was dissolved in an aqueous solution previously saturated with Sodium chloride (ca. 1.0 mL). To this solution, the heteropoly salt catalyst was added, followed by the addition of ethyl acetate (ca. 4. 0 mL). This tube was stirred and sealed, being then introduced microwave oven reactor (CEM Discovery microwave reactor), where the temperature was monitored through an internal probe.

At the end of the reaction, the tube was removed from the reactor and the organic phase was transferred to a flask containing anhydrous sodium sulfate. Then, it was filtered and transferred to a volumetric flask (ca. 5.0 mL), and its volume was checked with ethyl acetate. Finally, an aliquot (ca. 238 µL) of this solution was collected, the volume was completed to 1.0 mL with ethyl acetate solution containing 1,3,5-trimethoxybenzene (TMB) as an internal standard (i.e., TMB, 1.312 mg mL^{-1}).

The quantification of HMF yield was done with a calibration curve obtained through analysis of gas chromatography coupled to a mass spectrometer (Shimadzu GCMS-QP2010C Ultra GC-MS fitted with an Ultra Alloy 5 column, 30 m, ID 0.25 mm). Standard solutions were prepared in ethyl acetate, with concentrations of HMF varying from 0.25 to 2.0 mg mL^{-1} and with an internal standard at 1.0 mg mL^{-1}.

The chromatographic conditions were as follow: injector temperature (563 K), oven temperature (40 K/ 2 min), heating rate (30 K/ min), final temperature (523 K/ 1.0 min).

2.5. Catalyst recycling

The catalyst recycling was performed using the aqueous phase of the reaction, which contains water, NaCl, and soluble heteropoly salt. The first run was carried out with the selected conditions (i.e., fructose (ca. 0.25 mmol), heteropoly salt catalyst (ca. 10 mol %), NaCl saturated water (1 mL) and ethyl acetate solution (5.0 mL). The sealed glass tube containing this mixture was heated in a microwave reactor (ca. 413 K) and 17.5 min. At the end of this period, the system was cooled to room temperature and the ethyl acetate was removed. In that same tube, a new charge of fructose (0.25 mmol) and 4.0 mL of ethyl acetate was added. This system was taken back to the microwave reactor and this procedure was repeated three more times.

3. Results And Discussion

3.1. Characterization of heteropoly salts

The characterization of all the metal transition-exchanged catalysts used in this work was previously discussed by us in two previous papers; the first one [43], where the metal exchanged catalysts were used in glycerol esterification reactions, and the second one, where the Aluminum salts were used as catalysts in olefin oxidations [45]. However, in this work, to check if the catalysts were correctly synthesized, we carried out UV-Vis and infrared spectroscopy analyses, and acidity measurements. All the results are presented in the supplemental material (Figures 1SM to 9SM; Tables 1SM).

The typical absorption bands of the Keggin anion of $H_3PW_{12}O_{40}$ appeared at 1080, 990, 890, and 790 cm^{-1} wavenumbers, and were assigned to the vibrations υ_{ass} (P–O_a), υ_{ass} (W–O_d), υ_{ass} (W–O_b–W) and υ_{ass} (W–O_c–W) bonds, respectively [46, 47]. These bands appear practically at the same wavenumbers in the FT-IR spectra of meta-exchanged salts, indicating that the structure of the Keggin anion was preserved after the protons exchange. These data agree with the literature [43]. The absence of splitting in-band attributed to the vibration of the P-O bond assure that no lacunar anion was formed and that the primary structure remained almost intact after the synthesis. The same effect was observed when silicotungstic acid had its protons exchanged by the same actions used herein [48].

The main absorption bands that are typical of Keggin heteropolyanions were also observed in the infrared spectra of all the metal-exchanged phosphotungstic acids, as unequivocally demonstrated a comparison of their spectra with the phosphotungstic acid (Figure 1SM-3SM).

The UV spectra were recorded at the range of 200-750 nm, however, the main absorption bands only appeared within intervals 190-325 nm (Figure 2).

The UV spectra of these compounds display two characteristic absorption bands, attributed to the charge transfer from Oxygen atoms to Tungsten since that W atom has electronic configuration "d^0" [49]. The first, with maximum absorption placed at low wavenumber (ca. 190 nm) was assigned to the charge transfer from terminal Oxygen to Tungsten. This band was almost not affected by the presence of metal cations. Conversely, a second absorption band, noticed around 260 nm was assigned to charge transfer from bridges Oxygen atoms to W atom [50]. The maximum absorption was slightly toward red, mainly when in the presence of M^{3+} cations (Figure 2b).

In the supplemental material, we compared the UV-Vis spectra of three Keggin HPAs with Copper-exchanged salts (Figs. 4SM-9SM). While the Uv-Vis spectra of phospho- or silicotungstic acid and Copper salt catalysts are similar, with two bands absorption at 190 nm and 255 nm, the Molybdenum catalysts were different. Only a strong absorption band was noticed, at 220 nm wavelength, with a shoulder at 225 nm. Although this result agrees with the literature, which attributes this band at charge transfer from O^{2-} anions to Mo^{6+} cations (i.e., probably in bridges O_c-Mo-O_c, likewise in Tungsten heteropoly catalysts), we suppose that the absorption band involving charge transfer from terminal Oxygen atoms was also shifted toward lower wavelength, which is out of spectral range analyzed [51].

It is noteworthy that when metal-substituted polyoxometalates (POM) are synthesized removing an MO unit (M = W, Mo), a lacunar catalyst is generated, and when in this catalyst is introduced a metal cation into Keggin anion structure, metal-substituted POM salts are obtained, which are also very active photocatalysts (i.e., $[PW_{11}M^{2+}O_{39}]^{5-}$, M^{2+} = Mn, Fe, Co, Ni, Cu, Zn) [52]. In the UV-Vis spectra of these types of doped-metal heteropoly salts, the presence of the transition metal ions in octahedral coordination leads to risen "d-d" transitions absorption bands, in the region from 450 to 780 nm [53]. However, comparatively to the charge transfer bands, "d-d" transitions lead to very weak absorption bands. Consequently, to detect these bands highly concentrated solutions were prepared and their UV-Vis spectra are shown in Figure 3. Aiming for higher clarity, only the spectral region from 350 to 1000 nm was presented.

The absence of these bands in the spectra of phosphotungstic acid and their Aluminum phosphotungstate salt can be explained by the absence of "d" electrons. Conversely, the intensity and position depended on the metal cation. They were visible in the spectra of $Ni_{3/2}PW_{12}O_{40}$ (380-450 nm), $Cr_{3/2}PW_{12}O_{40}$ (530-650 nm), $Cu_{3/2}PW_{12}O_{40}$ (650-900 nm), $Co_{3/2}PW_{12}O_{40}$ (450-600 nm) [54–56]. The spectra of metal cations with d^5 configuration (Mn^{2+} and Fe^{3+} ions) do not show bands with a detectable intensity

The potentiometric titration curves of metal-exchanged phosphotungstate are presented in Figure 4. According to Pizzio et. al, the measurements of initial electrode potential (Ei) provide the acidity strength of acid sites: Ei > 100 mV (very strong acid sites), 0 < Ei < 100 mV (strong acid sites), 100 < Ei < 0 (weak acid sites), and Ei < 100 mV (very weak acid sites) [44]. All the synthesized catalysts presented Ei > 100 mV, indicating that they have very strong acid sites. However, they showed different values of Ei, which

can be ordered as follow: $FePW_{12}O_{40} \approx CrPW_{12}O_{40} > AlPW_{12}O_{40} > Co_{3/2}PW_{12}O_{40} \approx Cu_{3/2}PW_{12}O_{40} > Ni_{3/2}PW_{12}O_{40}$ $Mn_{3/2}PW_{12}O_{40}$. Expected, the trivalent metal cations were the highest strength of acidity.

All these catalysts have still Brønsted acidity since the Lewis metal cations can react with hydration water molecules present in the heteropolyanion. It can be confirmed by the absorption band placed at 1620 cm^{-1} wavenumber in the infrared spectra of these salts (Figure 1). In supplemental material, we showed the titration curves of Keggin heteropolyacids (Fig. 10SM). The titration curve of phosphotungstic acid (Figure 10SM) and their $AlPW_{12}O_{40}$ salt have a sharp decline after the addition of 0.8 mL of *n*-butylamine. Conversely, the other curves presented a different behaviour, some with a strong fall of potential at the beginning of titration (i.e., $Ni_{3/2}PW_{12}O_{40}$, $Mn_{3/2}PW_{12}O_{40}$, $Cu_{3/2}PW_{12}O_{40}$, $Co_{3/2}PW_{12}O_{40}$), and other with more gradual diminishing in the Ei value (i.e., $CrPW_{12}O_{40}$, $FePW_{12}O_{40}$). Nonetheless, all these curves presented two plateaus, suggesting the presence of sites with different acidity strengths. Literature has described that the presence of acidity in the neutral salts of Keggin HPAs is due to the coordination of metal cations to water molecules, which lead to a release of H^+ ions. In addition, we previously demonstrated that the metal cations thyself can consume *n*-butylamine, due to the presence of empty orbitals.

When we compared the titration curves of Keggin HPAs with those of Cooper exchanged salts (Figs. 10SM and 11SM), we conclude that this modification remarkably modifies the profile of curves; although the Ei values have undergone a slight lowering (ca. 50 mV, at maximum), all the three curves presented two plateaus at different regions, after the Cu(II) doping, suggesting that there now acidity sites with different strength.

3.2. Catalytic tests

3.2.1. Evaluation of different metal phosphotungstate catalysts in HMF synthesis

An initial screening aiming to verify the most active and selective catalyst in the conversion of fructose to HMF was performed, using reaction conditions previously described by the group [17]. The main results are shown in Figure 5. It is important to highlight that at this stage, the reaction conditions are not optimized to achieve the maximum yield. Our objective herein is to evaluate all the catalysts at the same conditions.

The HMF yields varied from 40 to 53%, being the reactions catalyzed by Chromium and Copper phosphotungstate salts those that demonstrate to be more efficient. Initially, we have expected that the catalysts with higher strength of acidity (i.e., with higher Ei values, Figure 4) will achieve higher HMF yields.

Interesting, although the $CrPW_{12}O_{40}$ catalyst has presented a strong acidity and its reaction has achieved also a high HMF yield, the reactions in the presence of $FePW_{12}O_{40}$ or $AlPW_{12}O_{40}$, which also showed a

high acidity strength, reached only lower yields (Figure 5). Surprisingly, $Cu_{3/2}PW_{12}O_{40}$ that had an Ei value almost equal to the Ei measured for $AlPW_{12}O_{40}$, suggesting that both have a similar acidity strength, achieved the highest yield. It suggests that probably the success of the reaction depend on the other aspects that may be beyond the acidity strength of the catalysts. As the basis of these results, we can conclude that although necessary, the Brønsted acidity strength should not be too strong, to prevent further rehydration of HMF, consequently, the strongest acid will not necessarily be the best catalyst [57].

It is noteworthy that this reaction occurs in an aqueous phase, therefore, we carried out pH measurements to verify the acidity of the reaction medium after adding the metal exchange salt catalyst (Table 2SM). The pH value of the solutions was 3.3 (i.e., $AlPW_{12}O_{40}$, $FePW_{12}O_{40}$), which were partially soluble, and 3.2. for all the other soluble salts. These very close pH values are a consequence of levelling effect of the water. The aqueous medium becomes acidic due to the hydrolysis of metal cations, which generate H_3O^+ cations (Equations 1 and 2).

$$M^{x+} + n\,H_2O \rightleftharpoons M(H_2O)n^{x+} \quad \text{(Equation 1)}$$

$$M(H_2O)n^{x+} + H_2O \rightleftharpoons [M(H_2O)_{n-1}(OH)]^{(x+)-1} + H_3O^+ \quad \text{(Equation 2)}$$

3.2.2. Mechanistic insights

It is natural to suppose that the protons should be the main players in these catalytic games and therefore act as the main active sites. Therefore, in Scheme 1 we propose a reaction pathway that can be useful to explain how they have risen into reaction medium and how they can participate in steps that leads to the conversion of fructose to HMF. However, the Copper phosphotungstate has no protons. The literature describes that transition metal salts can be hydrolyzed generating hydronium cations in aqueous solutions (Equations 1 and 2). We suppose that the same occurs with Copper phosphotungstate (Scheme 1). Afterwards, the reaction probably proceeds such as the typical Brønsted -acid-catalyzed reactions (Scheme 1).

The first step begins with protonation of the hydroxyl bound to the anomeric carbon of fructose, followed by the loss of a water molecule, and the formation of the oxonium ion (intermediate I, Scheme 1). Subsequently, water removes β-hydrogen from the oxonium ion, forming an enol (intermediate II, Scheme 1) that is in tautomeric equilibrium (keto-enol) (intermediate III, Scheme 1). From the intermediate aldehyde, there is the protonation of a second hydroxyl (intermediate IV, Scheme 1), followed by the loss of another water molecule, leading to the formation of an α,β-unsaturated aldehyde (intermediate V, Scheme 1). Finally, the protonation of the secondary hydroxyl (intermediate VI, Scheme 1), followed by the loss of a dehydration e leads to the formation of the HMF molecule (Scheme 1).

Gomes et al. previously evaluated the activity of phosphotungstic acid and their pure Cesium salts or supported on matrices such as MCM-41 silica mesoporous and conclude that although $H_3PW_{12}O_{40}$/ MCM-41 has been an efficient solid catalyst, it was less active than soluble acid [58]. They attributed this

highest activity the greatest strength of Brønsted acidity of HPA. Nonetheless, it is known that when a Lewis acidity site is introduced in the catalyst, a positive effect can occur. For instance, Lai et al. investigated the conversion of glucose to HMF and verified that the yield achieved in the presence of $Ag_3PW_{12}O_{40}$ was higher than that in the presence of $H_3PW_{12}O_{40}$ catalyst [31]. Those authors attributed this effect to the Lewis acidity of Ag^+ cations, which favour the isomerization of carbon skeletal of glucose to fructose, and consequently the HMF formation. Herein, as we are starting from the fructose, no isomerization is required.

Although the mechanism describes as the reaction proceed in the presence of H_3O^+ cations, remains obscure still how the Copper cations can directly participate in this reaction. As the basis of these results, we can conclude that in addition to participating in the generation of H_3O^+ cations, the metal cation itself should also play an essential role in the catalytic process, possibly, promoting the dehydration steps. Another possibility is the Copper heteropoly salt minimizes the formation of humins from the polymerization of HMF, increasing its yielding.

Therefore, we will proceed with our investigation for a better understanding of this catalytic system. Although the $CrPW_{12}O_{40}$ has been also very active, due to the highest HMF yield achieved in $Cu_{3/2}PW_{12}O_{40}$-catalyzed reaction, it was selected to assess the effect of other reaction variables.

3.2.3. Effect of heteropolyanion in the activity of Copper exchanged heteropolyacid salts in fructose dehydration to synthesize HMF

The fructose dehydration in a biphasic system was carried out in the presence of different HPAs, as well as in the presence of their Copper exchanged salts (Figure 6). All the reactions were assisted by microwaves radiation.

Regardless of the Keggin anion, the Copper exchanged salts were always more efficient than their precursor acid. It means the protons exchange by Copper had a positive effect on the activity of catalysts. Measurements of pH performed in the solution after the catalyst addition showed that as similar to the observed in the reactions with the other metal exchanged phosphotungstate salts the pH was always close to 3.2, excepted when $Cu_2SiW_{12}O_{40}$ was the catalyst. Once more, it is demonstrated that the presence of Copper had a key aspect, possibly more important than Brønsted acidity, since the solutions with the same pH achieved different yields (i.e., $Cu_{3/2}PMo_{12}O_{40}$, ca. 39% against $Cu_{3/2}PW_{12}O_{40}$, ca. 53%).

Another important conclusion is that the anion present in the Copper salt also plays a relevant role; even with an equal Copper content, the reactions in the presence of phosphotungstate or phosphomolybdate salts reached different HMF yields (ca. 39 and 53%, respectively, Figure 6). Probably, these heteropolyanions should act also to stabilize the protonated species generated during the process.

3.2.4. Effect of type of anion in the activity of Copper *salts in fructose dehydration reactions to synthesize HMF*

To investigate in more detail the impact of anion present in the Copper salt, reactions with different salts were performed and the main results are shown in Figure 7. The acids corresponding were also included for a better comparison.

In all the reactions, the Copper salts were more effective than respective Brønsted acids. Possibly, Brønsted acid catalysts can polymerize the HMF, reducing consequently its selectivity as well as its yield. In addition, we have found that Copper chloride or nitrate-catalyzed reactions achieved almost the same yield of HMF as Copper phosphotungstate. Although cheaper than phosphotungstate, these salts are more corrosive and can generate by-products due to the addition of chloride or nitrate ions to the HMF.

3.3. Evaluation of main reaction variables

To assess the influence of catalyst load on the HMF yield, all the other reaction parameters were kept constant (Figure 8).

An increase in the amount of catalyst had a positive effect on the yield of HMF until 10 mol %. It can be assigned to the increase of active sites in solution due to higher catalyst concentration. For catalyst load higher than 10 mol %, no beneficial effect was verified. It is possible that at these conditions the reaction equilibrium within the time interval evaluated has been achieved. Therefore, using 10 mol % of catalyst, the next step was investigating how the yield of HMF vary through time (Figure 9).

The HMF yield was gradually increasing when the reaction was carried through greater periods. However, the maximum yield was achieved in a time of 17.5 min of reaction. Reactions performed in longer periods leads to a lowering of the yield of HMF, probably due to its degradation to humins.

Another important parameter is the temperature of the reaction. It was not possible to evaluate temperatures above 413 K due to limitations of the MW reactor because when doing experiments at 423 K the ethyl acetate (boiling point is 350 K) was lost, due to high pressure in the system.

Figure 10 displays the results of the reaction performed at three heating levels (ca. 393, 403 and 413 K), in the biphasic system containing the soluble catalyst.

The yields considerably drop to 46% at 403 K and 10% at 393 K. Therefore, as the greatest yield was achieved at the highest temperature, it is evidence of the endothermic character of the reaction.

The composition of the biphasic system is an aspect that may drastically affect the reaction yield, mainly because although the reaction occurs in the aqueous phase, the organic phase acts extracting the product formed. To decrease the solubility of HMF in the aqueous solution and to favour its migration to the organic phase, the reaction is carried out in a saturated solution. Different salts can distinctly affect the ionic strength of an aqueous solution and consequently impact the reaction yield. Figure 11 show the HMF yields obtained in reactions with the aqueous phase saturated using different ionic compounds.

When no salt was used, only a poor yield of HMF was achieved (ca. 24%, Figure 11). This result can be explained by the salting-out effect [59, 60]. When a solution is saturated with ions, the solubility of other

solutes is compromised. These ions interact strongly with water molecules, through ion-dipole interactions, lowering the solubility of HMF in the aqueous medium. Consequently, this makes it migrate more efficiently to the extracting organic phase. This explains why all evaluated systems containing salts have a better yield for HMF, since that it is extracted more efficiently in their presence, and to avoid also parallel reactions that can occur in the aqueous phase [15, 21].

In general, the best results are observed for systems with the salts NaCl (ca. 81%) and KCl (ca. 67%), which indicates a better HMF extraction efficiency for systems containing the cations Na^+ and K^+. Conversely, in the solution saturated with LiCl, only a 49% yield was reached. It is expected that cations with smaller radium will be more efficient to saturate this solution, and consequent they can favour the HMF removal toward the organic phase.

The reactions carried out in solutions saturated with $CaCl_2$ or $MgCl_2$ achieved yields of ca. 41% and 37%, respectively; the yields were lower and the formation of humins was observed. This lower yield can be assigned to greater ionic radium of cations Ca^{2+} and Mg^{2+}, which require a higher water molecules number to be completely hydrated. As smaller the cation hydration radii, as greater the salting-out effect, which leads to greater HMF extraction efficiency and, consequently, a lower occurrence of parallel reactions in the aqueous phase [21, 59]. Interesting that this effect was not observed when compared to the HMF yield of NaCl and LiCl.

The polarity of the organic phase as well as the intermolecular forces existent can favour the removal of HMF from the aqueous phase. This effect was investigated using the conditions optimized and different organic solvents. The main results are shown in Figure 12.

The selection of the organic solvents used to compare with ethyl acetate was performed as the basis on the literature as follows: MIBK [19, 61], acetonitrile [62] and tetrahydrofuran [20, 63] (Figure 12).

The reactions carried out with ethyl acetate as organic phase continued to be that with the highest HMF yield (ca. 81%), followed by the acetonitrile (ca. 65%) and MIBK ones (ca. 60%). Among the organic solvents tested, tetrahydrofuran was the worst extractor, reaching the poorest yield of ca. 32%, which was also lower than the yield achieved in a system without the extraction phase (ca. 46% yield). The superior performance of ethyl acetate can be assigned to its lowest dielectric constant, and its low dipole moment (Table 4SM). Although no hydrogen bond can exist between ethyl acetate molecules and HMF molecules, their physical properties look to have a synergic effect that favours the extraction of these product molecules from an aqueous phase.

Finally, the possibility of reducing the volume of ethyl acetate used in the extraction was also evaluated. The extraction was done using different volumes (ca. 4.0, 3.0, 2.0 and 1.0 mL: Figure 13). It was found that a reduction of volume used to extract the HMF triggered a drop in yields. This can be explained by the limitation caused by decreasing the volume of the extracting phase, which restricts the amount of HMF extracted and this leads to parallel reactions in the reaction phase, such as HMF self-condensation reactions that produce humins [61].

3.4. Catalyst recycling

Aiming at minimal waste generation and making the process more sustainable and viable, according to the principles of green chemistry [64], the recycling of $Cu_{3/2}PW_{12}O_{40}$ was evaluated. To do it, a first experiment was carried out under optimized conditions (413 K, 17.5 minutes,10 mol % catalyst, 413 K, MW). At the end of the reaction period, the system was cooled, the ethyl acetate was removed. To the tube containing the aqueous phase ($Cu_{3/2}PW_{12}O_{40}$, NaCl) a new charge of fructose (0.25 mmol) and ethyl acetate (4 mL) was added. This system was taken back to the MW reactor. Figure 14 shows the main results.

Thus, the aqueous phase and the catalyst were recycled for another four cycles (Fig. 14). The catalyst activity presented a minimum decline within the five successive cycles of reuse, and HMF yield decreased only from 81 to 77%.

4. Conclusions

In this work, we evaluated the activity of metal-exchanged Keggin heteropolyacid salts as catalysts to produce HMF in microwave-assisted reactions carried out in a water-ethyl acetate biphasic system. Among the heteropolyacids and salts evaluated, $Cu_{3/2}PW_{12}O_{40}$ was the most active and selective catalyst. The effects of the main variables of reaction were assessed. Among the solvents investigated, ethyl acetate was the best choice, due to the lowest dipole moment and low dielectric constant, which demonstrated to be more important than hydrogen bonds existent in other solvents. Sodium chloride promoted the most efficient salting-out effect. At the optimized conditions (ca. 413 K, $Cu_{3/2}PW_{12}O_{40}$ (10 mol %), biphasic system (ethyl/acetate (4 mL) / NaCl saturated aqueous solution (1 mL)), an HMF yield of 81% was achieved after 15 min MWI. The best performance of $Cu_{3/2}PW_{12}O_{40}$ is a consequence of the Lewis acidity of Cu^{2+}, which allows that it can coordinate with the water molecules, consequently releasing H_3O^+ ions, as demonstrated by the pH measurements. These ions can promote fructose dehydration. However, comparing the superior performance of $Cu_{3/2}PW_{12}O_{40}$ with those achieved by heteropolyacids or mineral Bronsted acids, we can conclude that a great amount of H_3O^+ ions can compromise the HMF yield, probably due to the rehydration of fructose or humins formation. A comparison with other Copper salts allowed concluding that the Cu^{2+} cation plays an essential role in this reaction, nonetheless, once that different Copper heteropoly salts had different performances, it suggests that the anion plays also an important role. We suppose that anion should act to stabilize the protonated species formed during the reaction. This work may bring a new application of polyoxometalate salts, in particular, Copper phosphotungstate, a recyclable, water-soluble, and less corrosive catalyst in modern biorefinery, and open a new route where MW assisted reactions carried out in biphasic systems can make more sustainable and green the industrial processes for biomass conversion.

Declarations

Acknowledgements

The authors are grateful Fundação de Amparo à Pesquisa do Estado de Minas Gerais – Brazil (FAPEMIG), Conselho Nacional de Desenvolvimento Científico e Tecnológico - Brazil (CNPq) and Coordenação de Aperfeiçoamento de Pessoal de Nível Superior - Brasil (CAPES - Finance Code 001). MJS and SAF are supported by Research Fellowships from CNPq.

References

1. Mika LT, Cséfalvay E, Németh Á (2018) Catalytic Conversion of Carbohydrates to Initial Platform Chemicals: Chemistry and Sustainability. Chem Rev 118:505–613. https://doi.org/10.1021/acs.chemrev.7b00395
2. Hassan A, Ilyas SZ, Jalil A, Ullah Z (2021) Monetization of the environmental damage caused by fossil fuels. Environ Sci Pollut Res 28:21204–21211. https://doi.org/10.1007/s11356-020-12205-w
3. Besson M, Gallezot P, Pinel C (2014) Conversion of Biomass into Chemicals over Metal Catalysts. Chem Rev 114:1827–1870. https://doi.org/10.1021/cr4002269
4. David GF, Ríos-Ríos AM, de Fátima Â, Perez VH, Fernandes SA (2019) The use of p-sulfonic acid calix[4]arene as organocatalyst for pretreatment of sugarcane bagasse increased the production of levoglucosan. Ind Crops Prod 134:382–387. https://doi.org/10.1016/j.indcrop.2019.02.034
5. Castro GAD, Fernandes SA (2021) Microwave-assisted green synthesis of levulinate esters as biofuel precursors using calix[4]arene as an organocatalyst under solvent-free conditions. Sustain Energy Fuels 5:108–111. https://doi.org/10.1039/d0se01257b
6. Brar SK, Dhillon GS, Soccol CR (2014) Biotransformation of waste biomass into high value biochemicals. Springer. https://doi.org/10.1007/978-1-4614-8005-1
7. Corma Canos A, Iborra S, Velty A (2007) Chemical routes for the transformation of biomass into chemicals. Chem Rev 107:2411–2502. https://doi.org/10.1021/cr050989d
8. Yu IKM, Tsang DCW (2017) Conversion of biomass to hydroxymethylfurfural: A review of catalytic systems and underlying mechanisms. Bioresour Technol 238:716–732. https://doi.org/10.1016/j.biortech.2017.04.026
9. van Putten R-J, de Vries JG, van der Waal JC, de Jong E, Rasrendra CB, Heeres HJ (2013) Hydroxymethylfurfural, A versatile platform chemical made from renewable resources. Chem Rev 113:1499–1597
10. Kong QS, Li XL, Xu HJ, Fu Y (2020) Conversion of 5-hydroxymethylfurfural to chemicals: A review of catalytic routes and product applications, Fuel Process. Technol. 209 106528. https://doi.org/10.1016/j.fuproc.2020.106528
11. Rosatella AA, Simeonov SP, Frade RFM, Afonso CAM (2011) 5-Hydroxymethylfurfural (HMF) as a building block platform: Biological properties, synthesis and synthetic applications. Green Chem 13:754–793. https://doi.org/10.1039/c0gc00401d

12. Deng F, Amarasekara AS (2021) Catalytic upgrading of biomass derived furans. Ind Crops Prod 159:113055. https://doi.org/10.1016/j.indcrop.2020.113055
13. Takagaki A, Nishimura S, Ebitani K (2012) Catalytic Transformations of Biomass-Derived Materials into Value-Added Chemicals, Catal. Surv from Asia 16:164–182. https://doi.org/10.1007/s10563-012-9142-3
14. Abdelaziz OY, Al-Rabiah AA, El-Halwagi MM, Hulteberg CP (2020) Conceptual Design of a Kraft Lignin Biorefinery for the Production of Valuable Chemicals via Oxidative Depolymerization, ACS Sustain. Chem Eng 8:8823–8829. https://doi.org/10.1021/acssuschemeng.0c02945
15. Esteban J, Vorholt AJ, Leitner W (2020) An overview of the biphasic dehydration of sugars to 5-hydroxymethylfurfural and furfural: A rational selection of solvents using COSMO-RS and selection guides. Green Chem 22:2097–2128. https://doi.org/10.1039/c9gc04208c
16. Despax S, Maurer C, Estrine B, Le Bras J, Hoffmann N, Marinkovic S, Muzart J (2014) Fast and efficient DMSO-mediated dehydration of carbohydrates into 5-hydroxymethylfurfural. Catal Commun 51:5–9. https://doi.org/10.1016/j.catcom.2014.03.009
17. de Paiva Silva Pereira S, Oliveira Santana J, Varejão Â, de Fátima SA, Fernandes (2019) p-Sulfonic acid calix[4]arene: A highly efficient organocatalyst for dehydration of fructose to 5-hydroxymethylfurfural. Ind Crops Prod 138:111492. https://doi.org/10.1016/j.indcrop.2019.111492
18. Cao Q, Guo X, Yao S, Guan J, Wang X, Mu X, Zhang D (2011) Conversion of hexose into 5-hydroxymethylfurfural in imidazolium ionic liquids with and without a catalyst. Carbohydr Res 346:956–959. https://doi.org/10.1016/j.carres.2011.03.015
19. Román-Leshkov Y, Chheda JN, Dumesic JA (2006) Phase modifiers promote efficient production of hydroxymethylfurfural from fructose, Science (80-.). 312. 1933–1937. https://doi.org/10.1126/science.1126337
20. Tang J, Zhu L, Fu X, Dai J, Guo X, Hu C (2017) Insights into the Kinetics and Reaction Network of Aluminum Chloride-Catalyzed Conversion of Glucose in NaCl-H_2O/THF Biphasic System. ACS Catal 7:256–266. https://doi.org/10.1021/acscatal.6b02515
21. Saha B, Abu-Omar MM (2014) Advances in 5-hydroxymethylfurfural production from biomass in biphasic solvents. Green Chem 16:24–38. https://doi.org/10.1039/c3gc41324a
22. Da Silva MJ, Julio AA, Dorigetto FCS (2015) Solvent-free heteropolyacid-catalyzed glycerol ketalization at room temperature. RSC Adv 5:44499–44506. https://doi.org/10.1039/c4ra17090c
23. Gonçalves CE, Laier LO, Cardoso AL, Da MJ, Silva (2012) Bioadditive synthesis from $H_3PW_{12}O_{40}$-catalyzed glycerol esterification with HOAc under mild reaction conditions, Fuel Process. Technol. 102 46–52. https://doi.org/10.1016/j.fuproc.2012.04.027
24. Vilanculo CB (2021) Can Brønsted acids catalyze the epoxidation of allylic alcohols with H_2O_2 ? With a little help from the proton, the $H_3PMo_{12}O_{40}$ acid did it and well. 512:111780–111789. https://doi.org/10.1016/j.mcat.2021.111780

25. Da Silva MJ, Liberto NA (2016) Soluble and solid supported Keggin heteropolyacids as catalysts in reactions for biodiesel production: challenges and recent advances,1263–1283
26. Teixeira MG, Natalino R, da Silva MJ (2020) A kinetic study of heteropolyacid-catalyzed furfural acetalization with methanol at room temperature via ultraviolet spectroscopy. Catal Today 344:143–149. https://doi.org/10.1016/j.cattod.2018.11.071
27. Vilanculo CB, de Andrade Leles LC, da Silva MJ (2020) $H_4SiW_{12}2O_{40}$-Catalyzed Levulinic Acid Esterification at Room Temperature for Production of Fuel Bioadditives, Waste and Biomass Valorization. 11:1895–1904. https://doi.org/10.1007/s12649-018-00549-x
28. Yang Y, Abu-Omar MM, Hu C (2012) Heteropolyacid catalyzed conversion of fructose, sucrose, and inulin to 5-ethoxymethylfurfural, a liquid biofuel candidate. Appl Energy 99:80–84. https://doi.org/10.1016/j.apenergy.2012.04.049
29. Huang F, Su Y, Tao Y, Sun W, Wang W (2018) Preparation of 5-hydroxymethylfurfural from glucose catalyzed by silica-supported phosphotungstic acid heterogeneous catalyst. Fuel 226:417–422. https://doi.org/10.1016/j.fuel.2018.03.193
30. Liu A, Zhang Z, Fang Z, Liu B, Huang K (2014) Synthesis of 5-ethoxymethylfurfural from 5-hydroxymethylfurfural and fructose in ethanol catalyzed by MCM-41 supported phosphotungstic acid. J Ind Eng Chem 20:1977–1984. https://doi.org/10.1016/j.jiec.2013.09.020
31. Lai F, Yan F, Wang Y, Li C, Cai J, Zhang Z (2021) Tungstophosphoric acid supported on metal/Si-pillared montmorillonite for conversion of biomass-derived carbohydrates into methyl levulinate. J Clean Prod 314:128072. https://doi.org/10.1016/j.jclepro.2021.128072
32. Kumari PK, Rao BS, Padmakar D, Pasha N, Lingaiah N (2018) Lewis acidity induced heteropoly tungustate catalysts for the synthesis of 5-ethoxymethyl furfural from fructose and 5-hydroxymethylfurfural. Mol Catal 448:108–115. https://doi.org/10.1016/j.mcat.2018.01.034
33. Tang Y, Cheng Y, Xu H, Wang Y, Ke L, Huang X, Liao X, Shi B (2019) Binary oxide nanofiber bundle supported Keggin-type phosphotungstic acid for the synthesis of 5-hydroxymethylfurfural. Catal Commun 123:96–99. https://doi.org/10.1016/j.catcom.2019.02.015
34. da Silva MJ, da Silva Andrade PH, Ferreira SO, Vilanculo CB, Oliveira CM (2018) Monolacunary $K_8SiW_{11}O_{39}$-Catalyzed Terpenic Alcohols Oxidation with Hydrogen Peroxide. Catal Letters 148:2516–2527. https://doi.org/10.1007/s10562-018-2434-0
35. Srinivas M, Raveendra G, Parameswaram G, Prasad PSS, Lingaiah N (2016) Cesium exchanged tungstophosphoric acid supported on tin oxide: An efficient solid acid catalyst for etherification of glycerol with tert-butanol to synthesize biofuel additives. J Mol Catal A Chem 413:7–14. https://doi.org/10.1016/j.molcata.2015.10.005
36. Batalha DC, Ferreira SO, da Silva RC, da Silva MJ (2020) Cesium-Exchanged Lacunar Keggin Heteropolyacid Salts: Efficient Solid Catalysts for the Green Oxidation of Terpenic Alcohols with Hydrogen Peroxide, ChemSelect. 5:1976–1986. https://doi.org/10.1002/slct.201903437
37. da Silva MJ, Lopes NPG, Ferreira SO, da Silva RC, Natalino R, Chaves DM, Texeira MG (2020) Monoterpenes etherification reactions with alkyl alcohols over cesium partially exchanged Keggin

heteropoly salts: effects of catalyst composition. Chem Pap. https://doi.org/10.1007/s11696-020-01288-x

38. da Silva MJ, de Oliveira CM (2017) Catalysis by Keggin heteropolyacid salts. Curr Catal 7:26–34. https://doi.org/10.2174/2211544707666171219161414
39. Chaves DM, Ferreira SO, Da Silva RC, Natalino R (2019) José Da Silva, Glycerol Esterification over Sn(II)-Exchanged Keggin Heteropoly Salt Catalysts: Effect of Thermal Treatment Temperature. Energy and Fuels 33:7705–7716. https://doi.org/10.1021/acs.energyfuels.9b01583
40. Da Silva MJ, Vilanculo CB, Teixeira MG, Julio AA (2017) Catalysis of vegetable oil transesterification by Sn(II)-exchanged Keggin heteropolyacids: bifunctional solid acid catalysts. React Kinet Mech Catal 122:1011–1030. https://doi.org/10.1007/s11144-017-1258-z
41. Da Silva MJ, Julio AA, Ferreira SO, Da Silva RC, Chaves DM (2019) Tin(II) phosphotungstate heteropoly salt: An efficient solid catalyst to synthesize bioadditives ethers from glycerol. Fuel 254:115607–115618. https://doi.org/10.1016/j.fuel.2019.06.015
42. Pinheiro PF, Chaves DM, da Silva MJ (2019) One-pot synthesis of alkyl levulinates from biomass derivative carbohydrates in tin(II) exchanged silicotungstates-catalyzed reactions. Cellulose 26:7953–7969. https://doi.org/10.1007/s10570-019-02665-w
43. Da Silva MJ, Liberto NA, De Andrade Leles LC, Pereira UA (2016) Fe4(SiW12O40)3-catalyzed glycerol acetylation: Synthesis of bioadditives by using highly active Lewis acid catalyst. J Mol Catal A Chem 422:69–83. https://doi.org/10.1016/j.molcata.2016.03.003
44. Pizzio LR, Vázquez PG, Cáceres CV, Blanco MN (2003) Supported Keggin type heteropolycompounds for ecofriendly reactions. Appl Catal A Gen 256:125–139. https://doi.org/10.1016/S0926-860X(03)00394-6
45. da Silva MJ, de Andrade Leles LC, Ferreira SO, da Silva RC, de Viveiros K, Chaves DM, Pinheiro PF (2019) A Rare Carbon Skeletal Oxidative Rearrangement of Camphene Catalyzed by Al-Exchanged Keggin Heteropolyacid Salts, ChemistrySelect. 4:7665–7672. https://doi.org/10.1002/slct.201901025
46. Holclajtner-Antunović I, Mioč UB, Todorović M, Jovanović Z, Davidović M, Bajuk-Bogdanović D, Laušević Z (2010) Characterization of potassium salts of 12-tungstophosphoric acid. Mater Res Bull 45:1679–1684. https://doi.org/10.1016/j.materresbull.2010.06.064
47. Méndez L, Torviso R, Pizzio L, Blanco M (2011) 2-Methoxynaphthalene acylation using aluminum or copper salts of tungstophosphoric and tungstosilicic acids as catalysts. Catal Today 173:32–37. https://doi.org/10.1016/j.cattod.2011.03.028
48. da Silva MJ, Rodrigues AA (2020) Metal silicotungstate salts as catalysts in furfural oxidation reactions with hydrogen peroxide. Mol Catal 493:111104–111114. https://doi.org/10.1016/j.mcat.2020.111104
49. Combs-Walker LA, Hill CL (1991) Stabilization of the defect (“lacunary”) complex PMo11O397– isolation, purification, stability characteristics, and metalation chemistry. Inorg Chem 30:4016–4026. https://doi.org/10.1021/ic00021a010

50. Mandal S, Selvakannan PR, Pasricha R, Sastry M (2003) Keggin ions as UV-switchable reducing agents in the synthesis of Au core-Ag shell nanoparticles. J Am Chem Soc 125:8440–8441. https://doi.org/10.1021/ja034972t
51. Patel A, Patel J (2020) Nickel salt of phosphomolybdic acid as a bi-functional homogeneous recyclable catalyst for base free transformation of aldehyde into ester. RSC Adv 10:22146–22155. https://doi.org/10.1039/d0ra04119j
52. Liu CG, Zheng T, Liu S, Zhang HY (2016) Photodegradation of malachite green dye catalyzed by Keggin-type polyoxometalates under visible-light irradiation: Transition metal substituted effects. J Mol Struct 1110:44–52. https://doi.org/10.1016/j.molstruc.2016.01.015
53. Li Y, Zhang Y, Wu P, Feng C, Xue G (2018) Catalytic oxidative/extractive desulfurization of model oil using transition metal substituted phosphomolybdates-based ionic liquids. Catalysts 8:639–652. https://doi.org/10.3390/catal8120639
54. Kurajica S, Popović J, Tkalčec E, Gržeta B, Mandić V (2012) The effect of annealing temperature on the structure and optical properties of sol-gel derived nanocrystalline cobalt aluminate spinel. Mater Chem Phys 135:587–593. https://doi.org/10.1016/j.matchemphys.2012.05.030
55. Youn MH, Kim H, Song IK, Barteau KP, Barteau MA (2005) UV-visible spectroscopic study of solid state 12-molybdophosphoricacid catalyst, React. Kinet Catal Lett 87:85–91. https://doi.org/10.1007/s11144-006-0012-8
56. Mazari T, Marchal CR, Hocine S, Salhi N, Rabia C (2010) Oxidation of propane over ammonium-transition metal mixed keggin phosphomolybdate salts. J Nat Gas Chem 19:54–60. https://doi.org/10.1016/S1003-9953(09)60035-9
57. Guo X, Guo F, Li Y, Zheng Z, Xing Z, Zhu Z, Liu T, Zhang X, Jin Y (2018) Dehydration of D-xylose into furfural over bimetallic salts of heteropolyacid in DMSO/H_2O mixture. Appl Catal A Gen 558:18–25. https://doi.org/10.1016/j.apcata.2018.03.027
58. Gomes FNDC, Mendes FMT, Souza MMVM (2017) Synthesis of 5-hydroxymethylfurfural from fructose catalyzed by phosphotungstic acid. Catal Today 279:296–304. https://doi.org/10.1016/j.cattod.2016.02.018
59. Görgényi M, Dewulf J, Van Langenhove H, Héberger K (2006) Aqueous salting-out effect of inorganic cations and anions on non-electrolytes. Chemosphere 65:802–810. https://doi.org/10.1016/j.chemosphere.2006.03.029
60. Desai ML, Eisen EO (1966) Salt Effects in Liquid-Liquid Equilibria. J Chem Eng Data 11:480–484. https://doi.org/10.1021/je60049a021
61. Lucas N, Nagpure AS, Gurrala L, Gogoi P, Chilukuri S (2020) Efficacy of clay catalysts for the dehydration of fructose to 5-hydroxymethyl furfural in biphasic medium. J Porous Mater 27:1691–1700. https://doi.org/10.1007/s10934-020-00943-8
62. Wrigstedt P, Keskiväli J, Repo T (2016) Microwave-Enhanced Aqueous Biphasic Dehydration of Carbohydrates to 5-Hydroxymethylfurfural. RSC Adv 6:18973–18979. https://doi.org/10.1039/x0xx00000x

63. Fang X, Wang Z, Yuan B, Song W, Li S, Lin W (2018) Efficient conversion of cellulose to 5-hydroxymethylfurfural in $NaHSO_4/ZrO_2/H_2O$-THF biphasic system, ChemSelect. 3:12243–12249. https://doi.org/10.1002/slct.201802029
64. Sheldon RA (2017) The E factor 25 years on: The rise of green chemistry and sustainability. Green Chem 19:18–43. https://doi.org/10.1039/c6gc02157c

Scheme

Scheme 1 is available in the Supplemental Files section

Figures

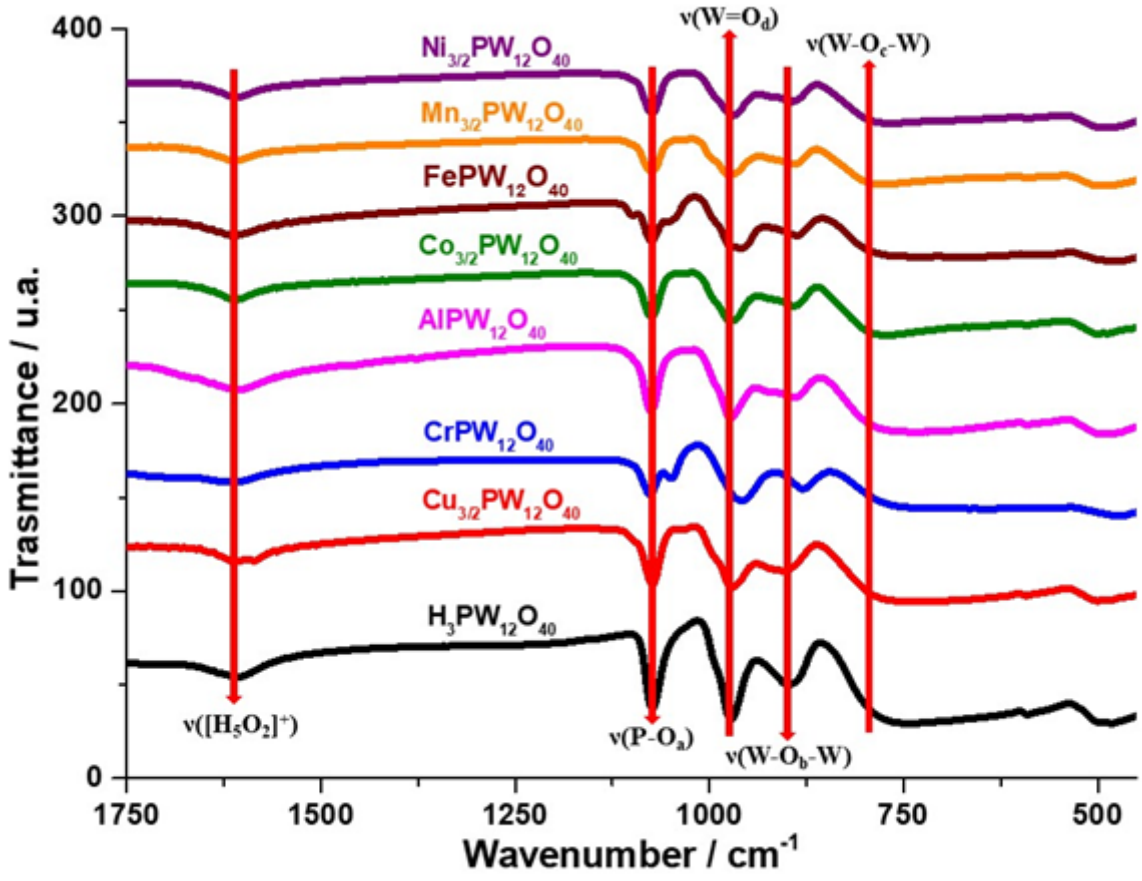

Figure 1

Comparison of infrared spectra of phosphotungstic acid and their metal exchanged salts

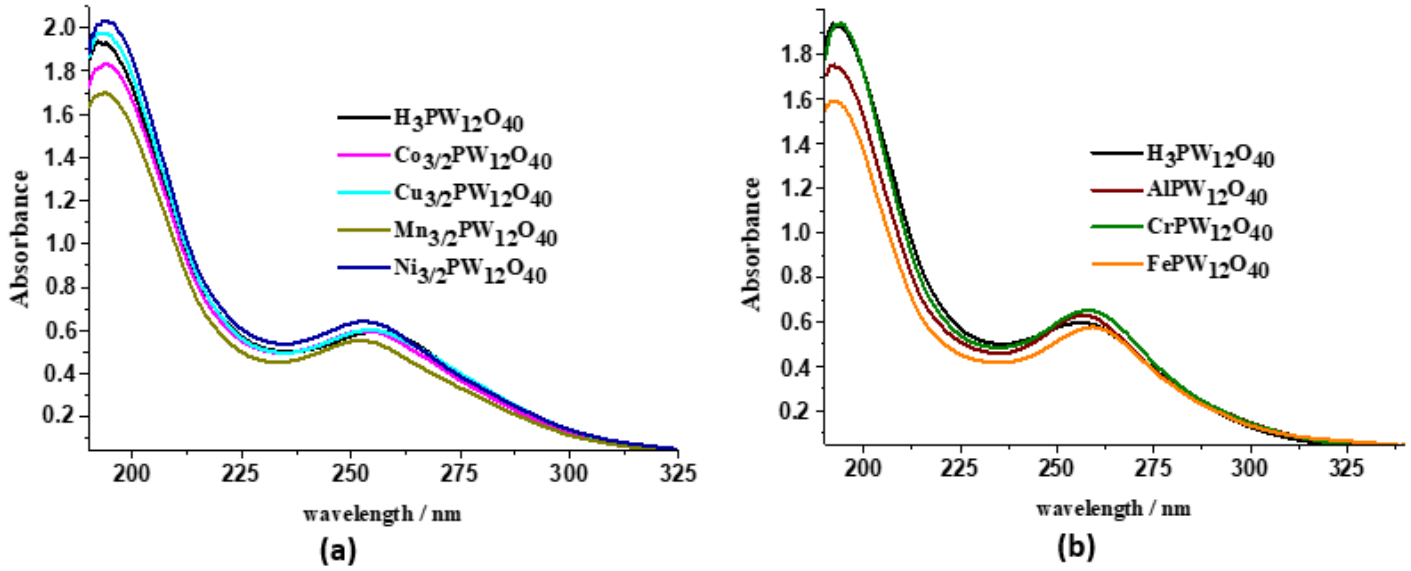

Figure 2

Comparison of UV spectra of phosphotungstic acid and their M2+ (a) and M3+ (b) metal exchanged salts

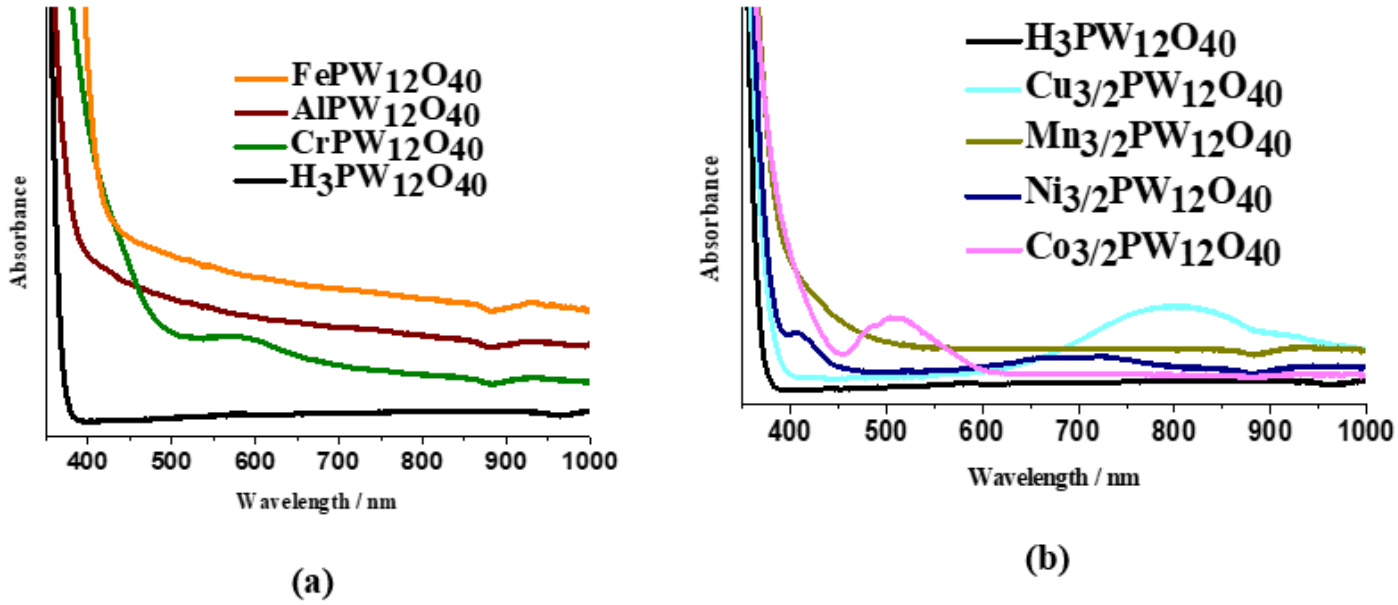

Figure 3

Comparison of Visible spectra of phosphotungstic acid and their M2+ (a) and M3+ (b) metal exchanged salts

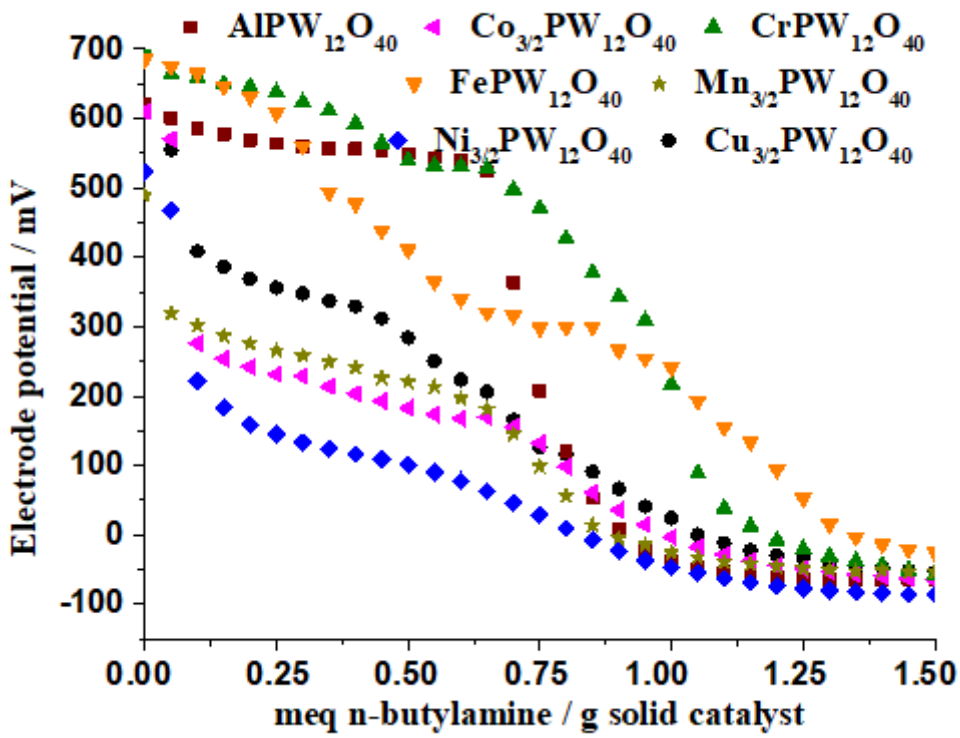

Figure 4

Curves of potentiometric titration with n-butylamine of metal-exchanged phosphotungstic acid.

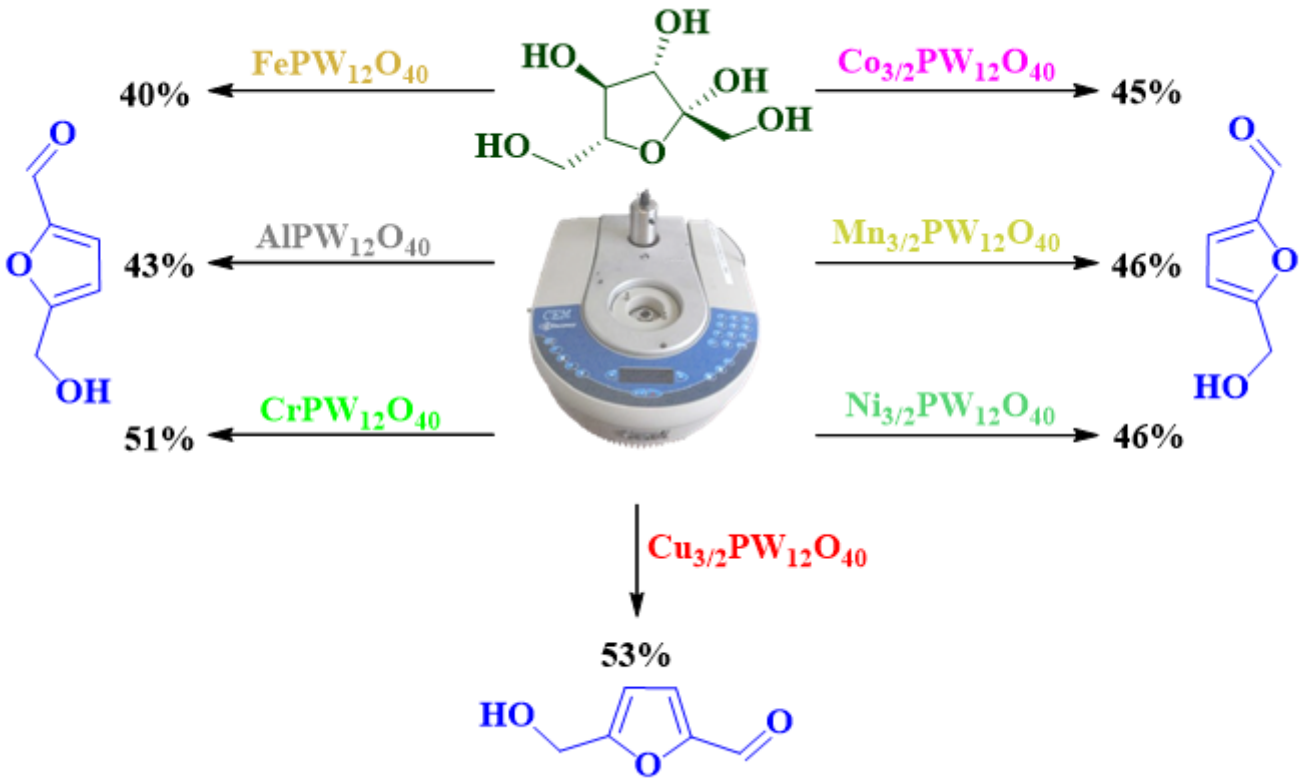

Figure 5

HMF yields (%) achieved in the metal phosphotungstate-catalyzed fructose dehydration reactionsa. aReaction conditions: fructose (0.25 mmol), catalyst (5 mol %), temperature (413 K), MW, biphasic system (AcOEt (4 mL)/ NaCl saturated aqueous solution (1mL)), time (10 min).

Figure 6

Effect of Keggin anion on the HMF yields (%) achieved in the heteropolyacid or Copper heteropolyacid-catalyzed fructose dehydration reactionsa. aReaction conditions: fructose (0.25 mmol), catalyst (5 mol %), temperature (413 K), microwaves irradiation, biphasic system (AcOEt (4 mL)/ NaCl saturated aqueous solution (1 mL)), time (10 min).

Figure 7

Yields of HMF achieved in Brønsted acid or Copper salt-catalyzed fructose dehydration reactionsa aReaction conditions: fructose (0.25 mmol), catalyst (5 mol %), temperature (413 K), MW, biphasic system (AcOEt/ NaCl saturated aqueous solution (4:1)), time (10 min).

Figure 8

Effect of catalyst load on the yield of HMF in Cu3/2PW12O40-catalyzed fructose dehydration reactionsa aReaction conditions: fructose (0.25 mmol), catalyst load (variable), temperature (413 K), MW, biphasic system (AcOEt (4 mL)/ NaCl saturated aqueous solution (1 mL)), time (10 min).

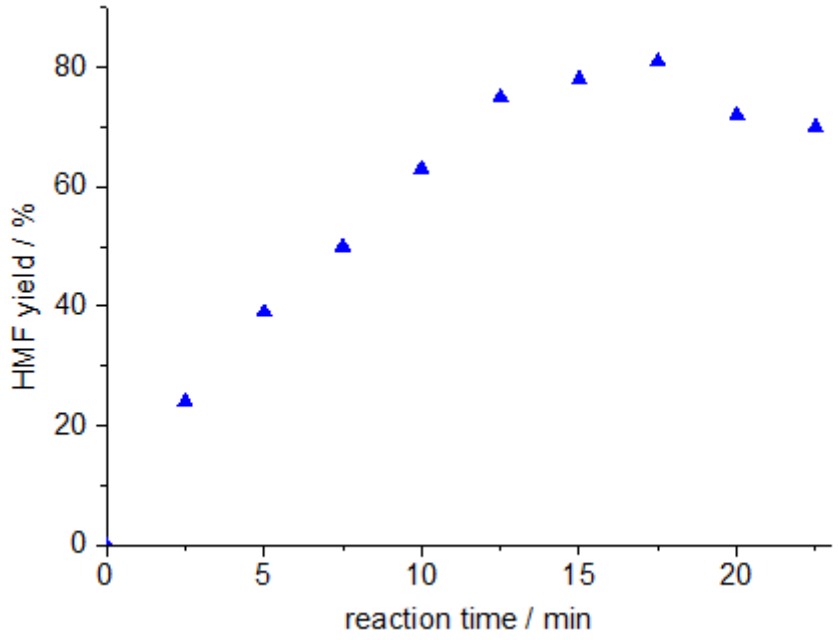

Figure 9

Variation of the HMF yield in Cu3/2PW12O40-catalyzed fructose dehydration reactions at different time periodsa aReaction conditions: fructose (0.25 mmol), catalyst load (10 mol %), temperature (413 K), MW, biphasic system (AcOEt (4 mL)/ NaCl saturated aqueous solution (1 mL)), time (variable).

Figure 10

Impact of temperature in the HMF yield in Cu3/2PW12O40-catalyzed fructose dehydration reactionsa aReaction conditions: fructose (0.25 mmol), catalyst load (10 mol %), temperature (variable), MW, biphasic system (AcOEt (4 mL)/ NaCl saturated aqueous solution (1 mL)), time (17.5 min).

Figure 11

Effect of salt present in the saturated aqueous solution on the HMF yield in Cu3/2PW12O40-catalyzed fructose dehydration reactionsa aReaction conditions: fructose (0.25 mmol), catalyst load (10 mol %), temperature (413 K), MW, biphasic system (AcOEt (4 mL)/ saturated aqueous solution (1 mL)), time (17.5 min).

Figure 12

Effect of organic phase on the HMF yield in Cu3/2PW12O40-catalyzed fructose dehydration reactionsa aReaction conditions: fructose (0.25 mmol), catalyst load (10 mol %), temperature (413 K), MW, biphasic system variable/ saturated aqueous solution (4:1), time (17.5 min).

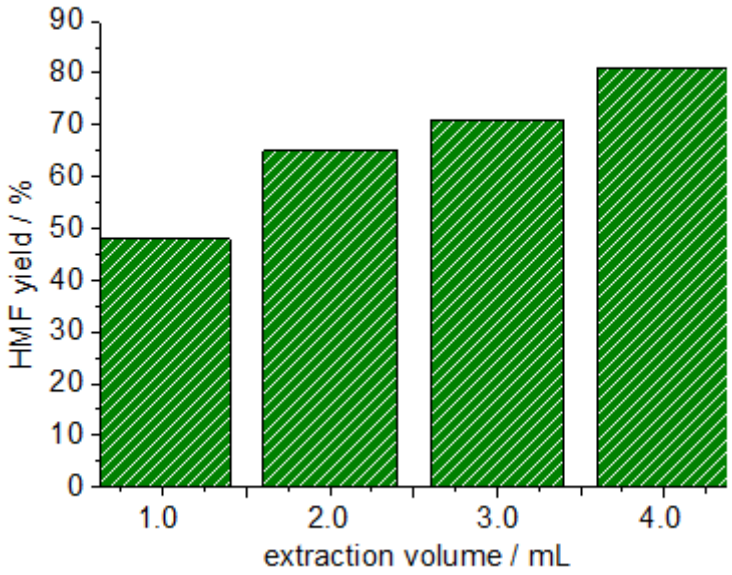

Figure 13

Effect of extraction volume on the HMF-yield in Cu3/2PW12O40-catalyzed fructose dehydration reactionsa aReaction conditions: fructose (0.25 mmol), catalyst load (10 mol %), temperature (413 K), MW, biphasic system (ethyl/acetate NaCl saturated aqueous solution), time (17.5 min).

Figure 14

Catalyst recycling in Cu3/2PW12O40-catalyzed fructose dehydration reactions. a Reaction conditions: fructose (0.25 mmol), catalyst load (10 mol %), temperature (413 K), MW, biphasic system (ethyl/acetate NaCl saturated aqueous solution), time (17.5 min).

Supplementary Files

This is a list of supplementary files associated with this preprint. Click to download.

- Scheme1.png
- SupportingInformation.docx
- Ga1.png